Available online at www.sciencedirect.com
SCIENCE DIRECT®

Journal of the European Ceramic Society 24 (2004) 2015–2021
www.elsevier.com/locate/jeurceramsoc

Interfacial reaction of TiO_2/NiCuZn ferrites in multilayer composites

Hsing-I Hsiang*, Wen-Chang Liao, Yu-Ju Wang, Ya-Fang Cheng

Department of Resources Engineering, National Cheng Kung University, Tainan, Taiwan, ROC

Received 9 January 2003; accepted 2 May 2003

Abstract

A composite layer device incorporating TiO_2 and NiCuZn ferrites has been developed. The cofiring behavior and interfacial interaction between TiO_2/NiCuZn ferrites at 900 °C were studied by using dilatometry, X-ray diffractometry (XRD), scanning electron microscopy (SEM) and energy dispersive X-ray spectroscopy (EDS). Intermediate layers were observed following the interfacial reaction between TiO_2 and PbO- or Bi_2O_3-doped NiCuZn ferrites. The intermediate layers were $PbTiO_3$ and $Bi_4Ti_3O_{12}$, respectively. But no intermediate layers were produced at the interface between TiO_2 and the V_2O_5-doped NiCuZn ferrites. The intermediate layers formed during cofiring resulted in delamination. Therefore, V_2O_5 should be recommended as a good sintering aid for NiCuZn ferrite in preparing TiO_2/NiCuZn ferrite composite layer devices.

Keywords: Cofiring; Ferrites; Interfacial reaction; $(Ni,Cu,Zn)Fe_4O_4$; TiO_2

1. Introduction

With the growing appetite for handheld electronic devices, these will undergo further miniaturization, reduction in weight and portability. Through the integration of inductors, capacitors and resistors into one monolithic chip component, the integrated component will offer better performance and save more occupied space on the printed circuit board during assembling. Therefore, the passive component will become a compact integrated passive component.[1]

TiO_2 and NiCuZn ferrites have been widely used in manufacturing capacitors and inductors due to their superior dielectric and magnetic properties. Ag is chosen as the material for the internal conductor for the multilayer chip inductors due to its low resistivity resulting in components with high quality factor. The melting point of Ag is 961 °C. Therefore, the ferrite is required to sinter at temperatures below 900 °C to prevent Ag diffusion into the ferrite that would increase the resistivity of the internal conductivity and damage the insulation resistivity of the ferrites. Improved densification of ceramics at low temperatures can be achieved by optimizing the powder morphology, adding glass flux and optimizing the sintering profile.[2,3] Of the above methods, lowering the sintering temperature by the addition of sintering aids is the most effective and least expensive technique. The attainment of a low sintering temperature (below 900 °C) and the magnetic properties of NiCuZn ferrites with different sintering aids have been accordingly studied extensively.[4–6] However, the reaction and diffusion between the TiO_2 and NiCuZn ferrites with such different sintering aids during cofiring has not yet been reported.

One of the most important processes in manufacturing defect-free multilayer chip LC devices involves the cofiring of capacitor and inductor materials at a low temperature. Mismatched densification kinetics and severe chemical reaction between the different materials could generate undesirable defects such as delamination, cracks and camber in the final products. In this study, the cofiring behavior and interfacial interaction between TiO_2/NiCuZn ferrites at 900 °C were studied. Through these investigations an effective sintering aid for NiCuZn ferrites in preparing TiO_2/NiCuZn ferrite multilayer composites could be suggested.

* Corresponding author. Tel.: +886-6-2757575x62821; fax: +886-6-2380421.
E-mail address: hsingi@mail.ncku.edu.tw (H.-I. Hsiang).

0955-2219/03/$ - see front matter © 2003 Elsevier Ltd. All rights reserved.
doi:10.1016/S0955-2219(03)00368-6

2. Experimental

The NiCuZn ferrites (Ni:Cu:Zn:Fe = 0.58:0.12:0.3:1.98) were prepared from reagent-grade NiO, CuO, ZnO and Fe_2O_3, which were mixed and then calcined at 740 °C for 2 h. The calcined NiCuZn ferrite powders were added to 3 wt.% of either PbO, Bi_2O_3 or V_2O_5 and then milled in a polyethylene bottle with YTZ balls for 24 h in an ethanol medium. The reagent grade TiO_2 (anatase phase) powder was mixed with 2 wt.% CuO in a polyethylene bottle with YTZ balls for 24 h using ethanol as medium. The NiCuZn ferrites and TiO_2 powders were dried in an oven and then separately added to PVA for granulation. The powders were separately cold-isostatic pressed at 200 MPa into pellets 1.0 cm in diameter and 0.28 cm in height. The TiO_2/NiCuZn ferrite composites were prepared by first pressing TiO_2 powder in a mold and then adding NiCuZn ferrite powders and pressing again, both at 62 MPa and then cold-isostatic pressing pairs of pellets at 200 MPa. The resulting samples were sintered at 900 °C for 2 h at a heating rate of 10 °C/min. The densities of the sintered samples were determined by the Archimedean method.

Densification curves from room temperature to 1100 °C were determined in air at a heating rate of 10 °C/min using a horizontal-loading dilatometer.

Phase transformation in the anatase specimens with and without CuO addition after calcining at different temperatures for 2 h was investigated by XRD. The crystallite sizes of the TiO_2 in these specimens were determined using the Scherrer equation.

The as-sintered TiO_2/NiCuZn ferrite composites were quenched into cold water to separate the interface by means the stresses produced by the different thermal expansion coefficients of the TiO_2 and NiCuZn ferrites. XRD (Siemens D5000), SEM (Hitahi S-4100) and EDS (Noran Voyager 2.0) were used to detect the interfacial reactions that occurred during cofiring.

3. Results and discussion

3.1. Effect of additives on the densification of NiCuZn ferrites

Fig. 1 shows the shrinkage curves of NiCuZn ferrites with different additives fired at a heating rate of 10 °C/min. The onset temperature of densification decreased to 550 °C for NiCuZn ferrites with 3 wt.% Bi_2O_3. Once it began to densify, the densification was completed at a higher densification rate over a narrower temperature range compared with samples having V_2O_5 and PbO additives. It had only one peak in the differential shrinkage rate (Fig. 2). The maximum densification rate for ferrites with 3 wt.% Bi_2O_3 occurred at about 780 °C and the densification completed at about 920 °C. For NiCuZn ferrites with additions of PbO and V_2O_5, the shrinkage onset temperatures were both shifted to about 650 °C and the densification completed at about 980 °C. Samples with V_2O_5 and PbO additions had two peaks in the differential shrinkage rate (Fig. 2). The linear shrinkages at 900 °C for samples with the addition of either Bi_2O_3, V_2O_5 or PbO were 17, 20 and 13%, respectively. The three additives promoted the densification of ferrites at 900 °C owing to the amount of the liquid phase and the good wetting during sintering.[4–6]

3.2. Effects of CuO addition on the phase transformation and densification of TiO_2

The XRD patterns of pure anatase calcined at 1000–1200 °C are shown in Fig. 3. It is found that the anatase to rutile (a→r-TiO_2) transformation started above 1100 °C being completed at 1200 °C. Fig. 4 shows the diffraction patterns of anatase with 2 wt.% CuO calcined at different calcination temperatures. A small

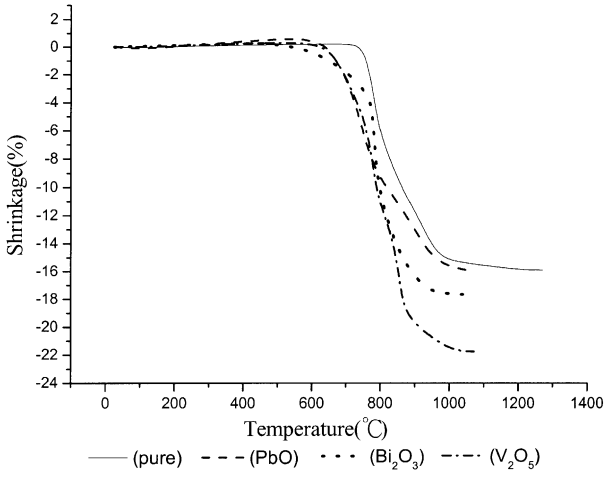

Fig. 1. The shrinkage curves of NiCuZn ferrites with different additives fired at a heating rate of 10 °C/min.

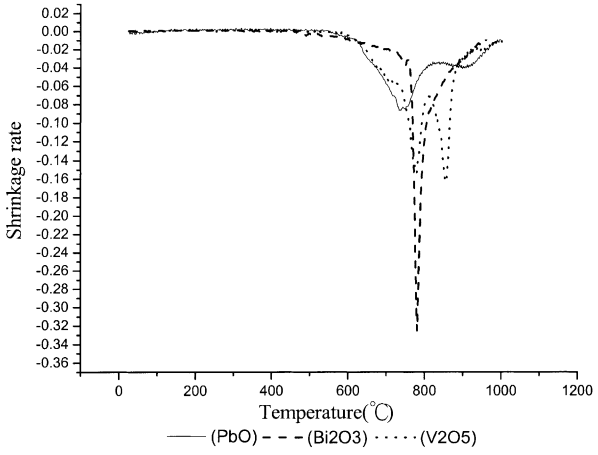

Fig. 2. The variations of shrinkage rate with temperature for PbO-, Bi_2O_3-, and V_2O_5-doped NiCuZn ferrites.

amount of rutile phase was observed in the sample calcined at 600 °C. At 800 °C, the anatase phase was fully transformed into rutile phase. The results revealed that most of the a→r-TiO_2 phase transformation for samples with CuO addition occurred at 600–800 °C.

Mackenzie[7] investigated the effect of additives on the anatase–rutile transformation. The incorporation of additives of valence lower than +4 accelerated transformation, because it provided a charge compensation mechanism by the formation of oxygen vacancies that enhanced the transport of atoms in the anatase structure, accelerating the phase transition.

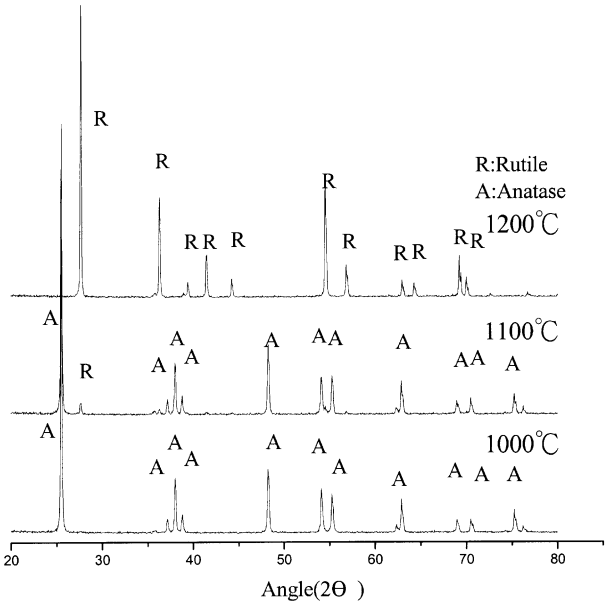

Fig. 3. The XRD patterns of pure anatase calcined at 1000–1200 °C.

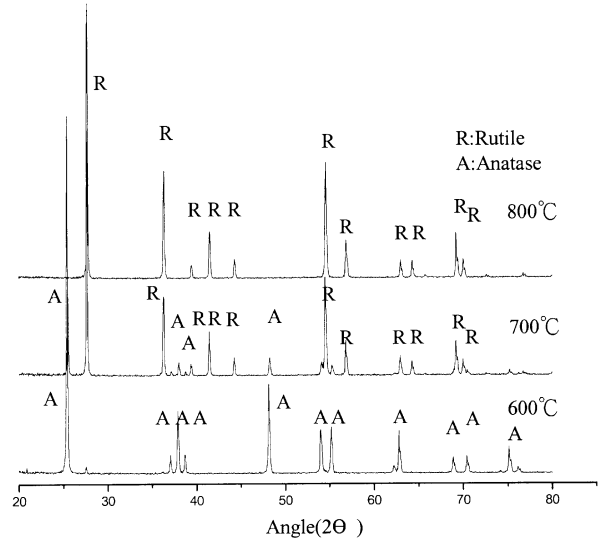

Fig. 4. The diffraction patterns of anatase with 2 wt.% CuO calcined at different calcination temperatures.

Fig. 5 shows the shrinkages of pure and CuO-doped anatase as a function of temperature at a heating rate of 10 °C/min. The shrinkage onset temperature of pure anatase was at about 900 °C. The sample did not complete densification even at 1100 °C. The onset shrinkage temperature of the sample with CuO addition decreased from 900 °C to about 700 °C, which is very close to the onset temperature of the a→r-TiO_2 phase transformation. Fig. 6 shows that the variation of shrinkage rate with temperature of CuO-doped TiO_2. It is observed that the differential shrinkage rate of CuO-doped TiO_2 exhibited two peaks around 800 and 986 °C. The first peak (800 °C) was connected with the a→r-TiO_2 phase transformation, whereas the second peak (986 °C) was related to the formation of a CuO-rich liquid phase as studied by Kim et al.[8] Consequently, the addition of CuO enhanced the a→r-TiO_2 phase transformation as well as densification.

A comparison between the densification behaviors of ferrites and anatase revealed that the sintering additives

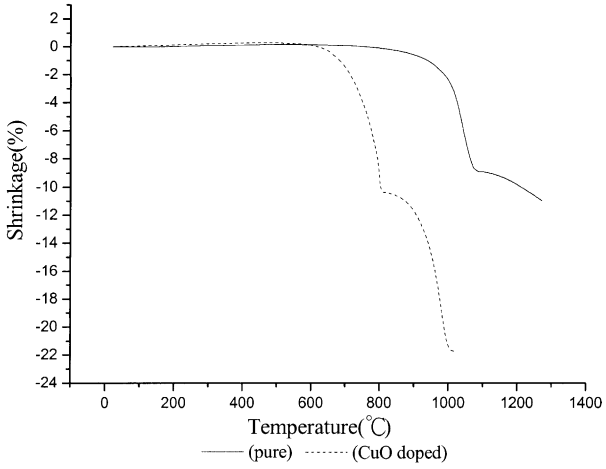

Fig. 5. The shrinkage of pure and anatase with 2 wt.% CuO as a function of temperature at a heating rate of 10 °C/min.

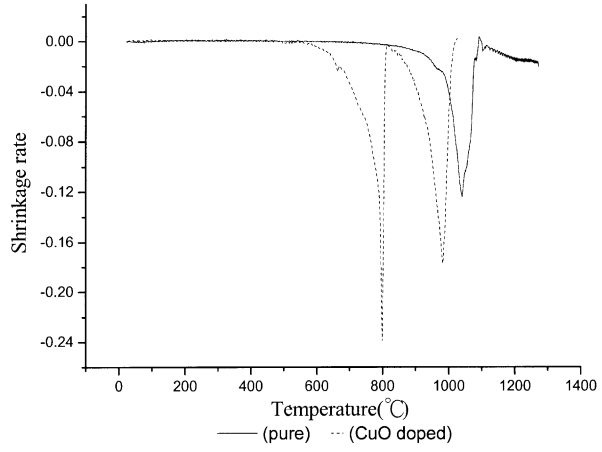

Fig. 6. The variation of shrinkage rate with temperature for pure and CuO-doped TiO_2.

could modify the mismatched sintering shrinkage between the two systems.

3.3. Interfacial reaction between NiCuZn ferrites with different additives and TiO_2

The X-ray diffraction patterns of the PbO-doped NiCuZn ferrites, CuO-doped TiO_2 and the interface region are shown in Fig. 7. It is observed that a second phase, $PbTiO_3$, appeared at the interface due to the chemical reaction between the PbO-doped ferrites and the TiO_2. The microstructure of the PbO-doped NiCuZn ferrites/TiO_2 interface is shown in Fig. 8. It is observed that there is formation of a flaky second phase. A quantitative analysis of the elementary composition in the second phase was investigated using EDS. The interfacial compound was identified as

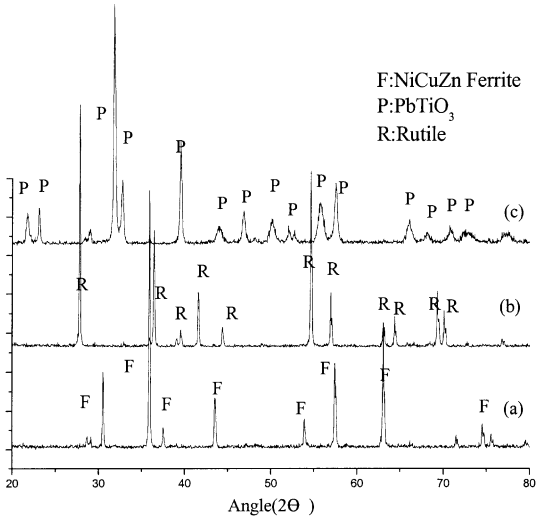

Fig. 7. The X-ray diffraction patterns of (a) the PbO-doped NiCuZn ferrites, (b) CuO-doped TiO_2 and (c) interface cofired at 900 °C.

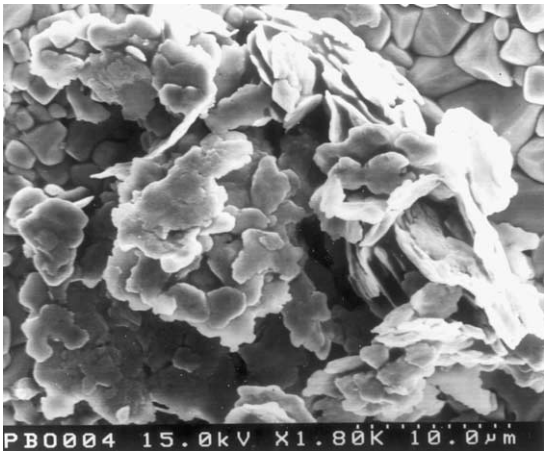

Fig. 8. The microstructure of the PbO-doped NiCuZn ferrites/TiO_2 interface cofired at 900 °C.

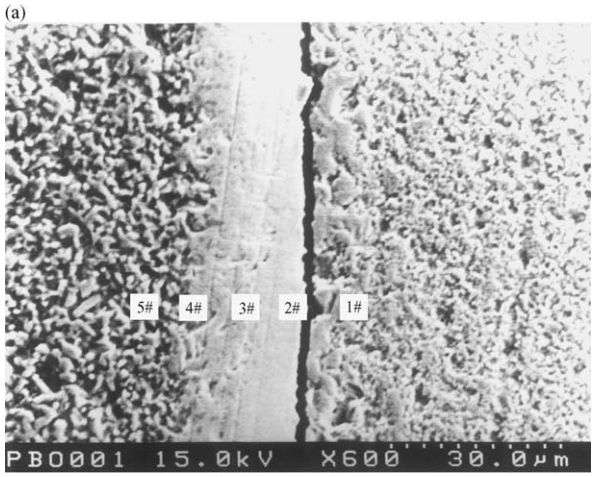

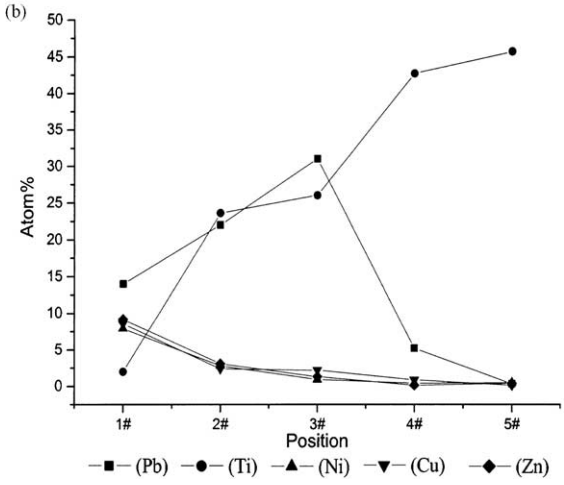

Fig. 9. (a) The cross-sectional view of the interface between PbO-doped NiCuZn ferrites and TiO_2 cofired at 900 °C. (b) The concentration profiles of the PbO-doped NiCuZn ferrites and TiO_2 fired at 900 °C.

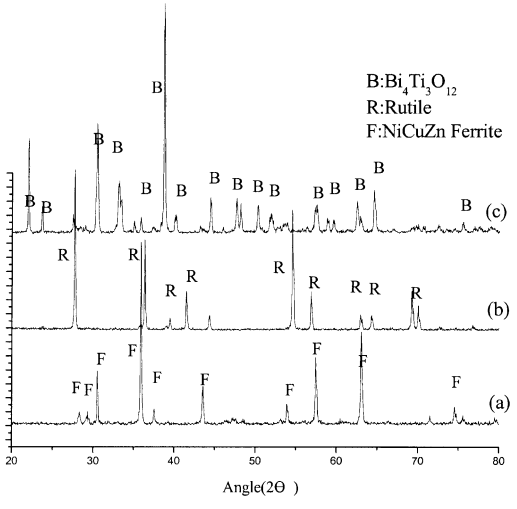

Fig. 10. The X-ray diffraction patterns of (a) the Bi_2O_3-doped NiCuZn ferrites, (b) CuO-doped TiO_2 and (c) interface cofired at 900 °C.

$PbTiO_3$ based on the EDS analysis. Fig. 9(a) shows the cross-sectional view of the interface between PbO-doped NiCuZn ferrites and TiO_2 cofired at 900 °C for 2 h. The numbers in the figure correspond to the position numbers in Fig. 9(b) where the concentrations detected with EDS are plotted. A Pb–Ti compound with Pb/Ti = 1/1 was detected at the interface, which coincides with the result of XRD (Fig. 7). It suggests that the PbO-rich glass dissolves TiO_2 and then $PbTiO_3$ is precipitated at the interface. The above result is in agreement with the phase diagram of PbO–TiO_2 (Ref. [9]) where a liquid phase coexists with $PbTiO_3$ at 900 °C.

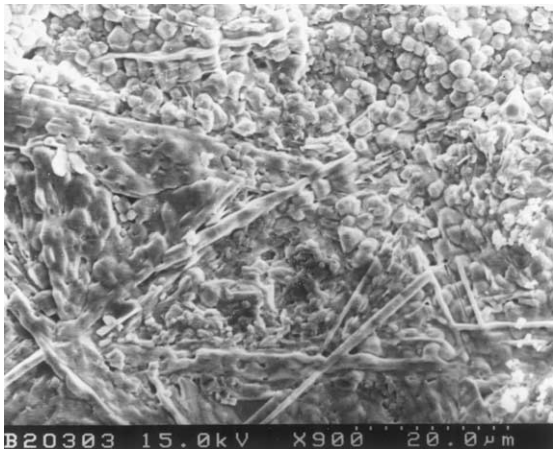

Fig. 11. The interfacial microstructure for Bi_2O_3-doped NiCuZn ferrites and TiO_2 cofired at 900 °C.

The X-ray diffraction patterns of the Bi_2O_3-doped NiCuZn ferrites, CuO-doped TiO_2 and interface are shown in Fig. 10. $Bi_4Ti_3O_{12}$ was found at the interface. Fig. 11 shows the interfacial microstructure for Bi_2O_3-doped NiCuZn ferrites and TiO_2. It is found that a second compound with needle morphology is formed at the interface. Judging from the quantitative analysis by EDS, the second phase was $Bi_4Ti_3O_{12}$. Fig. 12 shows the cross-sectional view of the interface between Bi_2O_3-doped NiCuZn ferrites and TiO_2 cofired at 900 °C for 2 h. The above results as shown in Figs. 11 and 12 suggest that the formation of a second phase can be explained by the dissolution of TiO_2 into a Bi_2O_3-rich glass and precipitation of $Bi_4Ti_3O_{12}$. Comparison of Figs. 9 and 12 suggests that the PbO-rich glass penetrated into the TiO_2 grain boundaries or incorporated into the TiO_2 lattice, whereas only a small amount of Bi could diffuse into the TiO_2 grain boundaries or lattice. From the

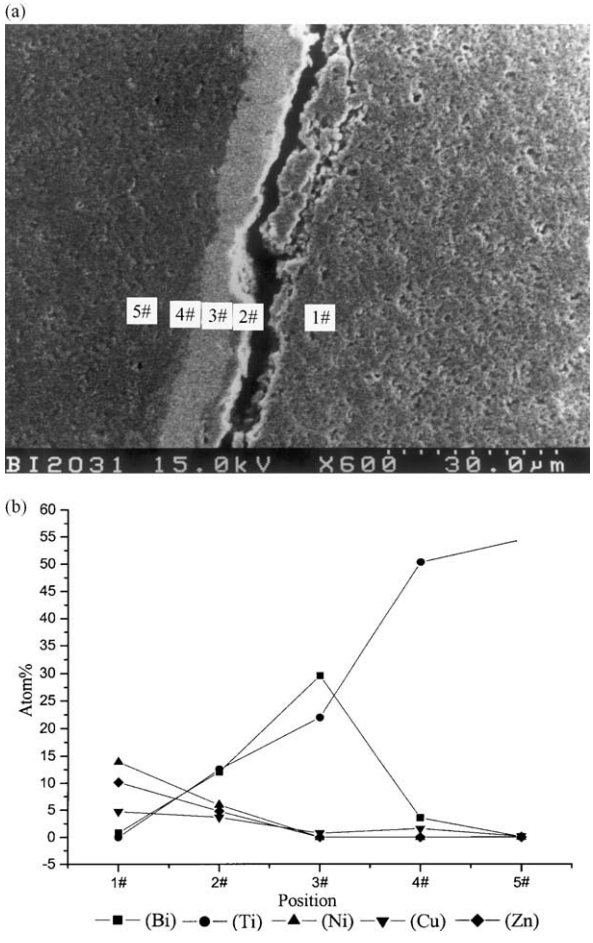

Fig. 12. (a) The cross-sectional view of the interface between Bi_2O_3-doped NiCuZn ferrites and TiO_2 cofired at 900 °C. (b) The concentration profiles of the Bi_2O_3-doped NiCuZn ferrites and TiO_2 fired at 900 °C.

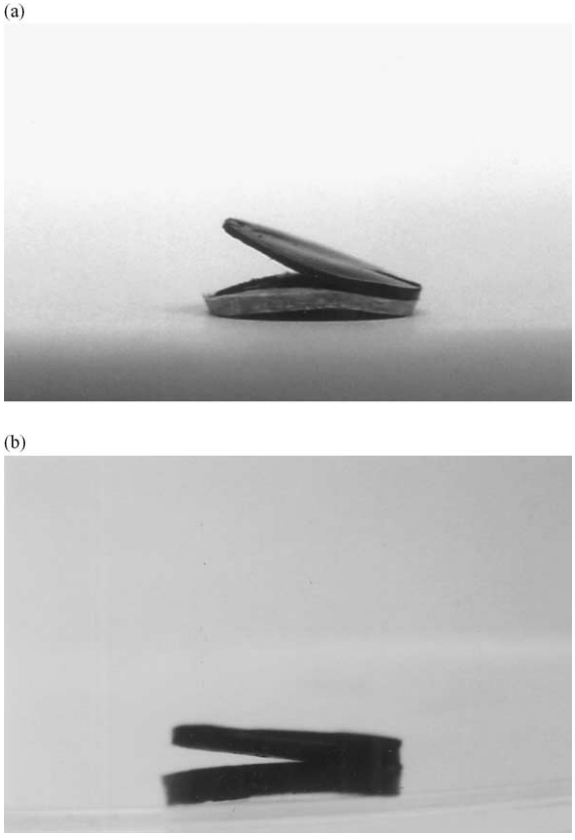

Fig. 13. Photographs of the (a) Bi_2O_3- or (b) PbO-doped NiCuZn ferrites/TiO_2 composites after firing at 900 °C.

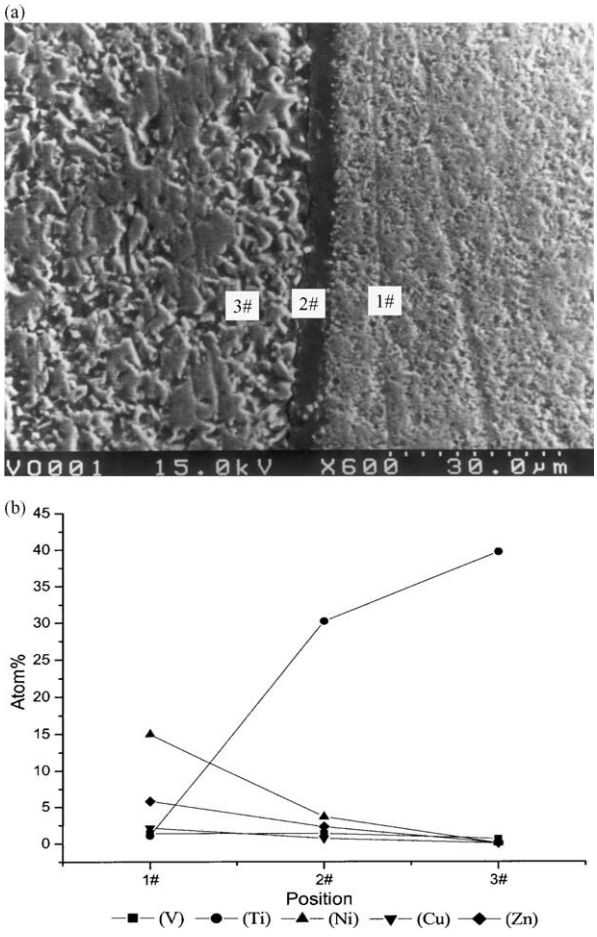

Fig. 14. (a) The concentration profiles of the V_2O_5-doped NiCuZn ferrites and TiO_2 fired at 900 °C. (b) The cross-sectional view of the interface between V_2O_5-doped NiCuZn ferrites and TiO_2 cofired at 900 °C.

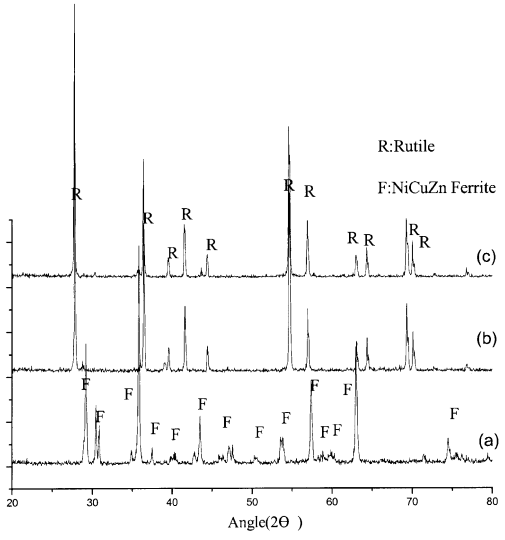

Fig. 15. The X-ray diffraction patterns of (a) the V_2O_5-doped NiCuZn ferrites, (b) CuO-doped TiO_2 and (c) interface cofired at 900 °C.

phase diagram of Bi_2O_3–TiO_2,[9] $Bi_4Ti_3O_{12}$ could coexist with liquid Bi_2O_3, which is consistent with the above result.

A second phase appeared at the interface due to the chemical reaction between Bi_2O_3- or PbO-doped NiCuZn ferrites and TiO_2 during cofiring. The intermediate layer formed during cofiring resulted in delamination (Fig. 13).

Fig. 14(a) shows the concentration profile of the V_2O_5-doped NiCuZn ferrites and TiO_2 fired at 900 °C for 2 h. No interfacial compound is observed at the interface. Unlike the ferrites doped with PbO and Bi_2O_3, the reaction layer cannot be detected in the XRD (Fig. 15) and EDS spectrum [Fig. 14(a)]. The above results are in agreement with the phase diagram of V_2O_5–TiO_2,[9] where the liquid phases of the mixed oxides coexist at 900 °C. Since no interfacial compounds were formed between V_2O_5-doped NiCuZn ferrites and TiO_2, it is evident that V_2O_5 is a promising sintering aid for NiCuZn ferrites in preparing TiO_2/NiCuZn ferrite composite layer devices.

4. Conclusion

1. Studies of additives for the densification of NiCuZn ferrites and anatase showed that these could correct the mismatched sintering shrinkage between the ferrites and anatase.
2. A second phase appeared at the interface due to the chemical reaction between Bi_2O_3- or PbO-doped NiCuZn ferrites and TiO_2 during cofiring. The intermediate layer formed during cofiring resulted in delamination.
3. Since no interfacial compounds were formed between V_2O_5-doped NiCuZn ferrites and TiO_2, V_2O_5 is a promising sintering aid for NiCuZn ferrites in preparing TiO_2/NiCuZn ferrite composite layer devices.

Acknowledgements

The author would like to express his thanks to the National Science Council of the Republic of China for financial support of this project (NSC91-2216-E-006-049).

References

1. Rector, J., Economic and technical viability of integral passives. In *The 48th IEEE Electronic Components and Technology Conference, Seattle*. 1998, pp. 218–224.
2. Nakamura, T., Low-temperature sintering of Ni–Cu–Zn ferrite and its permeability spectra. *J. Magn. Magn. Mater.*, 1997, **168**, 285–291.

3. Hsu, J. Y., Ko, W. S., Shen, H. D. and Chen, C. J., Low temperature fired NiCuZn ferrite. *IEEE Trans. Magn.*, 1994, **30**, 4875–4877.
4. Jean, J. H. and Lee, C. H., Effects of lead oxide on processing and properties of low-temperature-cofirable Ni–Cu–Zn ferrite. *J. Am. Ceram. Soc.*, 1999, **82**, 343–350.
5. Jean, J. H. and Lee, C. H., Low-fired NiO–CuO–ZnO ferrite with Bi_2O_3. *Jpn. J. Appl. Phys.*, 1999, **38**, 3508–3512.
6. Hsu, J. Y., Ko, W. S. and Chen, C. J., The effect of V_2O_5 on the sintering of NiCuZn ferrite. *IEEE Trans. Magn.*, 1995, **31**, 3994–3996.
7. MacKenzie, K. J. D., The calcination of titania: IV. The effect of additives on the anatase–rutile transformation. *Trans. J. Brit. Ceram. Soc.*, 1975, **74**, 29–34.
8. Kim, D. W., Kim, T. G. and Hong, K. S., Low-firing of CuO-doped anatase. *Mater. Res. Bull.*, 1999, **34**, 771–781.
9. Levin, E. M., Robbins, C. R. and McMurdie, H. F., *Phase Diagrams for Ceramists*. American Ceramic Society, Columbus, OH, 1987.